

Macrocyclic Rhodium(III) Hydrides and a Monomeric Rhodium(II) Complex

Andreja Bakac* and Leonard M. Thomas

Ames Laboratory and Chemistry Department, Iowa State University, Ames, Iowa 50011

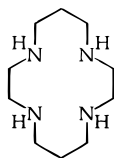
Received March 20, 1996[⊗]

Several mononuclear N₄-macrocyclic Rh(III) hydrides were prepared and characterized in the solid state and in solution. ¹H NMR, IR, and UV data are reported. The complex {*trans*-(Cl)([14]aneN₄)RhH}₂(ZnCl₄)·dmsO (**1**·dmsO) crystallizes in the triclinic system, space group *P* $\bar{1}$, in a unit cell of dimensions *a* = 10.680(3) Å, *b* = 13.460(3) Å, *c* = 14.277(4) Å, α = 86.49(2)°, β = 83.18(2)°, γ = 66.64(2)°. The data refined to a final value of *R* = 0.070 and *R*_w = 0.13 based on 2687 observed reflections. UV photolysis of chloride-free (H₂O)L¹RhH²⁺ results in homolytic Rh–H bond cleavage. The rhodium(II) product, L¹Rh(H₂O)²⁺, was characterized by ESR and UV spectroscopies. This species survives in acidic aqueous solution for over half an hour at room temperature. The photolysis of (H₂O)L¹RhH²⁺ in the presence of O₂ produces the superoxorhodium(III) ion, *trans*-L¹RhOO²⁺.

Introduction

Stable rhodium(II) complexes are typically dimeric, diamagnetic species.^{1–7} In exceptional cases,^{8–11} usually when the ligand bulk prevents formation of the Rh–Rh bond, monomeric Rh(II) is stable. Several such compounds containing sterically demanding porphyrins^{12–15} have recently been prepared and found to activate hydrocarbons by oxidative addition to two independent Rh(II) molecules. Dimeric Rh(II) porphyrins react by the same mechanism after an initial Rh–Rh bond cleavage. The C–H bond activation by a genuine monomeric Rh(II) is thus favored over the analogous reactions of Rh(II) dimers, where the energy of the Rh–Rh bond contributes to the overall thermodynamics. Some of the advantage may be lost, however, owing to the sensitivity of oxidative addition reactions to steric effects.

We initiated the present work with the idea that the much smaller but nonplanar saturated macrocycle [14]aneN₄ (L¹)



L¹

might introduce enough steric crowding around the rhodium center to destabilize the Rh–Rh bond. As a result, the rhodium(II) complex would be monomeric and a good candidate

for studies of reactivity toward a variety of substrates. There is very little information^{8,16–20} available on the chemistry of monomeric rhodium(II) complexes, especially those of non-porphyrin type, because they are usually transients generated by pulse radiolysis or flash photolysis. Such short-lived rhodium(II) can react only with the most reactive substrates or else decay¹⁶ or revert to the starting material.^{18–20}

As part of this work, we have prepared several novel hydrides of Rh(III) and used them both as reagents in thermal chemistry and as photochemical precursors of the corresponding Rh(II) complexes. The known²¹ cationic (NH₃)₅RhH²⁺ was also used in some of the work, but its use was limited by ligand exchange and dimerization reactions of the reduced form, (NH₃)₄(H₂O)-Rh²⁺.

Experimental Section

Materials. *cis*- and *trans*-[L¹RhCl₂]Cl,²² [(NH₃)₅RhH](SO₄),²¹ and [(NH₃)₄(H₂O)RhH](SO₄)²¹ were prepared by published procedures.

The synthesis of {*trans*-[(Cl)L¹RhH]}₂(ZnCl₄) (**1**) was carried out by a modification of the published procedure for the preparation of [(NH₃)₅RhH](SO₄).²¹ A 0.93 g sample of *trans*-[L¹Rh(Cl)₂]Cl was dissolved in 30 mL of H₂O. Then 3 mL of concentrated HCl was added, and the solution was thoroughly degassed with a stream of argon and warmed to 60 °C. Finally, 300 mg of Zn powder was added gradually over a period of ~2 min. The reaction mixture was stirred for an additional 2–3 min until the yellow color of *trans*-[L¹RhCl₂]Cl disappeared. After the mixture was cooled, the unreacted zinc was removed by filtration, and the colorless solution evaporated almost to dryness under vacuum. The solid **1** was filtered and washed with acetone. Analogous preparative procedure with the *cis*-chloro precursor yielded {*cis*-[(Cl)L¹RhH]}₂(ZnCl₄).

{*trans*-[(Cl)L¹RhD]}₂(ZnCl₄) was obtained by the same procedure as the protio compound, except that the preparation was carried out in D₂O.

Recrystallization of **1** from aqueous HCl yielded a snow-white product that is either *trans*-[(H₂O)L¹RhH](ZnCl₄) or *trans*-[(ZnCl₄)L¹-RhH]. We cannot distinguish with certainty between the two formulations on the basis of elemental analysis, because the molecular weights

[⊗] Abstract published in *Advance ACS Abstracts*, September 1, 1996.

- (1) Felthouse, T. R. *Prog. Inorg. Chem.* **1982**, 29, 73.
- (2) Maspero, F.; Taube, H. *J. Am. Chem. Soc.* **1968**, 90, 7361.
- (3) Dunbar, K. R. *J. Am. Chem. Soc.* **1988**, 110, 8247.
- (4) Bunn, A. G.; Wei, M.; Wayland, B. B. *Organometallics* **1994**, 13, 3390.
- (5) Van Voorhees, S. L.; Wayland, B. B. *Organometallics* **1987**, 6, 204.
- (6) Ogoshi, H.; Setsune, J.; Yoshida, Z. *J. Am. Chem. Soc.* **1977**, 99, 3869.
- (7) Weber, J. H.; Schrauzer, G. N. *J. Am. Chem. Soc.* **1970**, 92, 726.
- (8) Billig, E.; Shupack, S. I.; Waters, J. H.; Williams, R.; Gray, H. B. *J. Am. Chem. Soc.* **1964**, 86, 926.
- (9) Anderson, D. J.; Eisenberg, R. *Inorg. Chem.* **1994**, 33, 5378.
- (10) Bianchini, C.; Laschi, F.; Ottaviani, M. F.; Peruzzini, M.; Zanello, P.; Zanobini, F. *Organometallics* **1989**, 8, 893.
- (11) Harrowfield, J. M.; Herlt, A. J.; Lay, P. A.; Sargeson, A. M. *J. Am. Chem. Soc.* **1983**, 105, 5503.
- (12) Wayland, B. B.; Sherry, A. E.; Poszmik, G.; Bunn, A. G. *J. Am. Chem. Soc.* **1992**, 114, 1673.
- (13) Sherry, A. E.; Wayland, B. B. *J. Am. Chem. Soc.* **1989**, 111, 5010.
- (14) Wayland, B. B.; Ba, S.; Sherry, A. E. *J. Am. Chem. Soc.* **1991**, 113, 5305.

- (15) Wayland, B. B.; Sherry, A. E.; Bunn, A. G. *J. Am. Chem. Soc.* **1993**, 115, 7675.
- (16) Lillie, J.; Simic, M. G.; Endicott, J. F. *Inorg. Chem.* **1975**, 14, 2129.
- (17) Espenson, J. H.; Tinner, U. *J. Organomet. Chem.* **1981**, 212, C43.
- (18) Tinner, U.; Espenson, J. H. *J. Am. Chem. Soc.* **1981**, 103, 2120.
- (19) Howes, K. R.; Bakac, A.; Espenson, J. H. *Inorg. Chem.* **1988**, 27, 3147.
- (20) Howes, K. R.; Bakac, A.; Espenson, J. H. *Inorg. Chem.* **1989**, 28, 579.
- (21) Thomas, K.; Osborn, J. A.; Powell, A. R.; Wilkinson, G. *J. Chem. Soc. A* **1968**, 1801.
- (22) Bounsall, E. J.; Koprach, S. R. *Can. J. Chem.* **1970**, 48, 1481.

Table 1. Crystallographic Data for $\{trans-[Cl]([14]aneN_4)RhH\}_2(ZnCl_4) \cdot dmsO$ (**1**·dmsO)

empirical formula: $C_{22}H_{56}Cl_6N_8ORh_2SZn$
color, habit: clear, rectangular
cryst syst: triclinic
space group: $P\bar{1}$
unit cell dimens
$a = 10.680(3) \text{ \AA}$
$b = 13.460(3) \text{ \AA}$
$c = 14.277(4) \text{ \AA}$
$\alpha = 86.49(2)^\circ$
$\beta = 83.18(2)^\circ$
$\gamma = 66.64(2)^\circ$
$V = 1870.6(9) \text{ \AA}^3$
$Z = 2$
$fw = 964.73$
$d(\text{calc}) = 1.695 \text{ Mg/m}^3$
abs coeff = 12.509 mm^{-1}
radiation: Cu K α ($\lambda = 1.54178 \text{ \AA}$)
$T = 293(2) \text{ K}$
scan type: $2\theta - \theta$
θ range: = $3.12 - 56.88^\circ$
index ranges:
$-10 \leq h \leq 11$
$-1 \leq k \leq 14$
$-15 \leq l \leq 15$
no. of reflns collcd: 5795
no. of indep reflns: 5023 ($R_{\text{int}} = 0.0614$)
no. of obsd reflns ($I \geq 2\sigma(I)$): 2687
final R indices [$I \geq 2\sigma(I)$]: $R1^a = 0.0695$, $wR2^b = 0.1318$
R indices (all data): $R1^a = 0.1318$, $wR2^b = 0.1857$
GooF, ^c obsd and all data: 1.065, 0.888
weighting scheme: $w = \text{calc } w = 1/[\sigma^2(F_o^2) + (0.0800P)^2 + 0.0000P]$
where $P = (F_o^2 + 2F_c^2)^3$

^a $R1 = \sum ||F_o| - |F_c|| / \sum |F_o|$. ^b $wR2 = \sum [w(F_o^2 - F_c^2)^2] / \sum [w(F_o^2)^2]$ ^{0.5}, where $w = 1/[\sigma^2(F_o^2) + (aP)^2 + bP + d + e \sin \theta]$. ^c GooF = $[\sum [w(F_o^2 - F_c^2)^2] / (n - p)]^{0.5}$.

of the two compounds differ by only ~3% (one molecule of water). It is clear, however, that the recrystallized compound does not contain coordinated chloride ions. The product was filtered and dried in a vacuum desiccator at room temperature. Anal. Calcd for $[ZnCl_4]L^1-RhH$: C, 23.48, H, 4.93, N, 10.95, Rh, 20.12, Cl, 27.73, Zn, 12.78. Calcd for $[(H_2O)L^1RhH](ZnCl_4)$: C, 22.68, H, 4.76, N, 10.58, Rh, 19.44, Cl, 26.78, Zn, 12.35. Found (Desert Analytics): C, 23.53, H, 4.85, N, 10.70, Rh, 20.78, Cl, 27.64, Zn, 12.39. The agreement between calculated and experimental values is somewhat better for $(ZnCl_4)L^1-RhH$.

For photochemical and chemical experiments, all the hydrides were purified by ion-exchange on Sephadex SP-C25 to remove chloride and zinc ions. As explained later, this was necessary because chloride ions altered the outcome of photochemical experiments. Approximately 200 mg of the desired $[(Cl)L^1RhH]_2(ZnCl_4)$ was dissolved in 35 mL of 0.02 M HClO₄ and loaded onto the resin. The resin was rinsed with 0.02 M HClO₄ to remove chloride ions (AgNO₃ test). All the complexes behaved as 2+ ions and were eluted with 0.25 M HClO₄. This result confirms that both free and coordinated chloride ions were removed by ion-exchange. Solutions of all the rhodium hydrides prepared in this manner were analyzed for rhodium by inductively coupled plasma. The solution species most likely contain a molecule of H₂O in the remaining axial position, so that the complete formula is $trans-(H_2O)L^1-RhH^{2+}$. The coordinated water will be omitted hereafter.

Crystals of **1**·dmsO for X-ray diffraction were obtained by diffusion of acetone vapor into an acidic (HCl) solution of the complex in dmsO. A number of crystals were screened, but only a few diffracted significantly. The best one was chosen for data collection. The crystallographic data are summarized in Table 1. Three-dimensional intensity data were collected on a Siemens P4RA diffractometer with a graphite monochromator at room temperature. The crystal had the dimensions $0.2 \times 0.1 \times 0.05 \text{ mm}$, and was mounted in a glass capillary. Unit cell constants were determined from reflections found from a rotation photograph. The stability of the crystal was monitored by measuring three check reflections out of every 100 reflections. A 10% loss of intensity was observed in the course of data collection. Because

Table 2. ¹H NMR and IR Data for Rhodium Hydride Complexes

compound ^a	δ/ppm ($J_{\text{Rh-H}}/\text{Hz}$) ^b	Rh-H stretch/ cm^{-1}
$c-[(Cl)L^1RhH](ZnCl_4)_{0.5}$	-20.70 (36.4)	2119
$t-[(Cl)L^1RhH](ZnCl_4)_{0.5}$	-20.34 (34.4)	2124
$t-[(Cl)L^1RhD](ZnCl_4)_{0.5}$		1530
$[(NH_3)_3RhH](SO_4)$	-17.1 (14.5) ^d	2084
		2079 ^d
$[(ND_3)_3RhD](SO_4)$		1486 ^d
$t-[(NH_3)_4(H_2O)RhH](SO_4)$		2150
		2146 ^d

^a $L^1 = [14]aneN_4$, $c = \text{cis}$, and $t = \text{trans}$. ^b In dmsO containing 0.2 M CF₃SO₃H. ^c Solid state. ^d Reference 21.

of further degradation of the crystal after data collection, azimuthal scans could not be completed and no absorption correction was applied.

The $P\bar{1}$ space group was chosen on the basis of the lack of any systematic absences, and intensity statistics. The structure determination was done by use of direct methods in SHELXTL-Plus. All non-hydrogen atoms were placed directly from the E -map and subsequently refined with anisotropic displacement parameters. All hydrogen atom positions were treated as riding atoms with individual isotropic displacement parameters. The least-squares refinement was done using SHELXTL-93.²³ All calculations were done on a VAX Station 3100 computer using SHELXTL-Plus (Siemens Analytical Xray, Inc., Madison, WI) and SHELXTL-93.

Solutions of $trans-L^1Rh^{2+}$ and $trans-L^1RhO_2^{2+}$ for ESR spectrometry were prepared by photolysis of ~1 mM $trans-L^1RhH^{2+}$ in 0.01 M HClO₄ under argon and oxygen, respectively. The solutions were transferred to 5 mm ESR tubes and frozen in liquid nitrogen, and the spectra were collected at 120 K.

IR data were obtained by use of a Bio-Rad Digilab FTS-60A FT-IR spectrometer equipped with an MTEC Model 200 photoacoustic cell. Other spectroscopic data were obtained by use of a Shimadzu 3100 UV-visible spectrophotometer, Bruker 400 (NMR) and Bruker ER 200 D-SRC (ESR). Laser flash photolysis measurements used an Applied Photophysics instrument equipped with a Nd:YAG laser described earlier.²⁴ The excitation wavelength was 266 nm. Steady-state photolyses were carried out with 254 nm light produced in a Rayonet UV reactor.

Results and Discussion

All the syntheses were carried out under similar conditions and they all yielded white powdered hydrides. On the basis of the crystal structure of **1**·dmsO, we assume that the initial products of all the preparations were the tetrachlorozincate salts. The exact nature of the anion (Cl^- vs $0.5 ZnCl_4^{2-}$) in the solid state is, however, of minor importance because the anion should have little effect on the spectroscopic data for the cationic hydrides, and all of the chemistry was conducted in ion-exchanged aqueous perchlorate solutions in the absence of both zinc and chloride.

Spectroscopy. Rhodium-hydride stretching frequencies, Table 2, appear in the expected region, as shown by comparison with the known ammine complexes. The band at 2124 cm^{-1} disappeared when the preparation of **1** was carried out in D₂O and a new band, which we assign as a Rh-D stretch, appeared at 1530 cm^{-1} .

¹H NMR spectra were run in dmsO-*d*₆ containing 0.2 M CF₃SO₃H. We added the acid as a precautionary measure, because acidic conditions greatly stabilize aqueous solutions of the hydrides. The same may or may not be true for dmsO solutions.

The hydride resonances appear as doublets at $< -20 \text{ ppm}$, Table 2 and Figure 1. *cis*- and *trans*-(Cl)L¹RhH²⁺ each show only a single hydride signal, indicating that both complexes are

(23) Sheldrick, G. M. Shelex 93. Program for the Refinement of Crystal Structures. University of Göttingen, Germany.

(24) Huston, P.; Espenson, J. H.; Bakac, A. *J. Am. Chem. Soc.* **1992**, *114*, 9510.

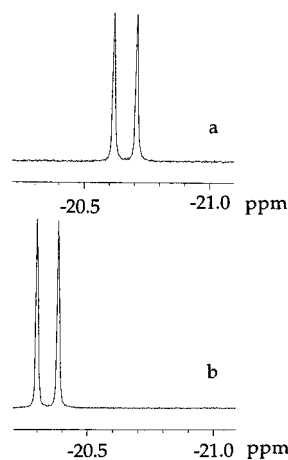


Figure 1. Rh–H region in the ^1H NMR spectra of (a) *cis*- $\text{L}^1(\text{Cl})\text{-RhH}^+$ (δ –20.70 ppm, $J_{\text{Rh-H}} = 36.4$ Hz) and (b) *trans*- $\text{L}^1(\text{Cl})\text{RhH}^+$ (δ –20.34 ppm, $J_{\text{Rh-H}} = 34.4$ Hz) in d_6 -dmsol containing 0.1 M $\text{CF}_3\text{SO}_3\text{H}$.

Table 3. UV Spectral Data for Rhodium Hydrides^a

complex ^b	λ_{max} ($\epsilon/\text{M}^{-1}\text{cm}^{-1}$)
<i>t</i> -(H_2O) L^1RhH^+	288 (470)
<i>c</i> -(H_2O) $\text{L}^1\text{RhH}^{2+}$	284 (507)
<i>t</i> -(NH_3) $_4(\text{H}_2\text{O})\text{RhH}^{2+}$	300 (298)
	300 (280) ^c
(NH_3) $_5\text{RhH}^{2+}$	307 ^c

^a In acidic aqueous solutions. ^b $\text{L}^1 = [14]\text{aneN}_4$, *c* = *cis*, and *t* = *trans*. ^c Reference 21.

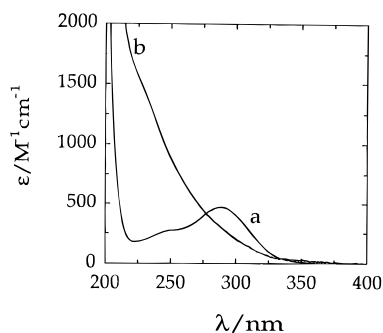


Figure 2. UV spectrum of *trans*- $\text{L}^1\text{RhH}^{2+}$ ($\text{L}^1 = [14]\text{aneN}_4$) in 0.1 M HClO_4 (a) before and (b) after photolysis at 254 nm under argon. Molar absorptivities in part b were calculated under the assumption that the conversion of $\text{L}^1\text{RhH}^{2+}$ to L^1Rh^{2+} was quantitative.

single isomers; i.e., no isomerization took place during the preparation of the hydrides from the dichloro complexes.

The UV spectral data in dilute aqueous perchloric acid are given in Table 3. All the complexes show a moderately strong band at ~ 290 -nm and a shoulder at ~ 250 nm, as shown for *trans*- $\text{L}^1\text{RhH}^{2+}$ in Figure 2. As discussed later, UV photolysis results in homolytic Rh–H bond cleavage.

Crystal Structure. A significant number of rhodium hydrides are known, but structural data have been reported for only a few such complexes.^{25–27} To the best of our knowledge, no macrocyclic rhodium hydride has been structurally characterized.

Positional parameters are given in Table 4, and selected bond lengths and angles are given in Tables 5 and 6. The asymmetric unit contains two similar rhodium cations, a tetrachlorozincate anion, and a molecule of dmsol, Figure 3. Only two formulas

Table 4. Atomic Coordinates ($\times 10^4$)^a and Equivalent Isotropic Displacement Parameters ($\text{\AA}^2 \times 10^3$)^b for $\{\text{trans}-[(\text{Cl})([14]\text{aneN}_4)\text{RhH}]\}_2(\text{ZnCl}_4)\cdot\text{dmsol}$ ($\mathbf{1}\cdot\text{dmsol}$)

atom	x	y	z	<i>U</i> (eq)
Rh(1)	3399(1)	9265(1)	1678(1)	43(1)
Rh(2)	1182(1)	5675(1)	3001(1)	42(1)
Cl(1)	3635(4)	7947(3)	3071(3)	52(1)
Cl(2)	1534(4)	3970(3)	3961(3)	54(1)
N(1)	3107(13)	8255(11)	766(8)	56(3)
N(2)	1379(13)	10149(11)	2009(9)	60(4)
N(3)	3678(13)	10298(10)	2556(9)	58(4)
N(4)	5439(13)	8381(10)	1324(9)	56(3)
N(5)	–319(12)	5448(10)	2385(8)	53(3)
N(6)	–108(12)	6559(10)	4101(9)	51(3)
N(7)	2655(12)	5935(10)	3631(8)	50(3)
N(8)	2484(14)	4834(11)	1875(9)	56(4)
C(1)	1999(17)	7918(14)	1103(13)	69(5)
C(2)	647(16)	8883(15)	1271(12)	64(5)
C(3)	504(17)	9558(14)	2126(13)	69(5)
C(4)	1222(16)	10798(12)	2870(11)	54(4)
C(5)	2305(18)	11205(13)	2711(11)	66(5)
C(6)	4859(19)	10590(14)	2243(12)	74(6)
C(7)	6178(16)	9645(14)	2062(14)	67(5)
C(8)	6309(18)	8964(15)	1209(13)	75(6)
C(9)	5628(18)	7697(16)	509(12)	75(6)
C(10)	4479(19)	7294(14)	633(12)	75(6)
C(11)	–1675(16)	6314(14)	2427(12)	66(5)
C(12)	–2198(16)	6723(15)	3420(13)	68(5)
C(13)	–1487(17)	7309(13)	3868(12)	69(5)
C(14)	649(17)	7078(13)	4563(12)	63(5)
C(15)	2083(17)	6314(14)	4580(11)	60(5)
C(16)	4052(17)	5018(14)	3564(13)	69(5)
C(17)	4571(17)	4613(16)	2552(13)	78(6)
C(18)	38455(17)	4054(13)	2088(13)	66(5)
C(19)	1711(19)	4278(13)	1459(12)	75(6)
C(20)	273(19)	5068(14)	1424(12)	67(5)
Zn(1)	8296(2)	3087(2)	1366(1)	47(1)
S(1)	6571(7)	459(5)	4481(4)	97(2)
O(1)	6528(16)	–128(12)	5378(9)	107(5)
Cl(3)	8392(4)	3548(4)	2860(3)	62(1)
Cl(4)	7351(4)	1816(3)	1496(3)	64(1)
Cl(6)	10436(4)	2347(3)	574(3)	56(1)
Cl(7)	7030(4)	4549(3)	526(3)	59(1)
C(102)	5259(19)	1789(16)	4616(13)	96(7)
C(101)	7978(21)	835(19)	4451(15)	116(8)

^a The estimated standard deviations in the parentheses are for the least significant digit. ^b Equivalent isotropic *U* defined as one-third of the trace of the orthogonalized U_{ij} tensor.

Table 5. Selected Bond Distances (\AA) for $\{\text{trans}-[(\text{Cl})([14]\text{aneN}_4)\text{RhH}]\}_2(\text{ZnCl}_4)\cdot\text{dmsol}$ ($\mathbf{1}\cdot\text{dmsol}$)

Rh(1)–Cl(1)	2.549(3)	Rh(1)–N(3)	2.056(13)
Rh(1)–N(1)	2.058(13)	Rh(1)–N(4)	2.043(12)
Rh(1)–N(2)	2.020(13)		

Table 6. Selected Bond Angles (deg) for $\{\text{trans}-[(\text{Cl})([14]\text{aneN}_4)\text{RhH}]\}_2(\text{ZnCl}_4)\cdot\text{dmsol}$ ($\mathbf{1}\cdot\text{dmsol}$)

N(2)–Rh(1)–N(4)	179.2(5)	C(1)–N(1)–Rh(1)	114.7(10)
N(1)–Rh(1)–N(3)	178.8(5)	C(10)–N(1)–Rh(1)	105.6(10)
N(2)–Rh(1)–N(1)	94.9(5)	C(3)–N(2)–C(4)	111.5(13)
N(4)–Rh(1)–N(1)	84.8(5)	C(3)–N(2)–Rh(1)	116.2(10)
N(2)–Rh(1)–N(3)	84.7(5)	C(4)–N(2)–Rh(1)	108.1(9)
N(4)–Rh(1)–N(3)	95.5(5)	C(6)–N(3)–Rh(1)	114.6(11)
N(2)–Rh(1)–Cl(1)	95.3(4)	C(5)–N(3)–Rh(1)	104.6(9)
N(4)–Rh(1)–Cl(1)	85.5(4)	C(8)–N(4)–Rh(1)	116.6(11)
N(1)–Rh(1)–Cl(1)	93.0(4)	C(9)–N(4)–Rh(1)	110.1(10)
N(3)–Rh(1)–Cl(1)	88.1(4)		

fit this result, $[\text{L}^1(\text{Cl})\text{Rh}^{\text{III}}\text{H}]^+$ and $[\text{L}^1(\text{Cl})\text{Rh}^{\text{II}}]^+$. The latter can be ruled out by a number of experimental facts, including the stability of the material in air. Most importantly, when the crystals are redissolved in H_2O , the UV spectrum of the rhodium hydride is obtained. We are thus confident that the material is indeed the hydridorhodium(III) complex. The hydride ligand

(25) Varshney, A.; Gray, G. M. *J. Organomet. Chem.* **1990**, 393, 415.

(26) Coyle, B. A.; Ibers, J. A. *Inorg. Chem.* **1972**, 11, 1105.

(27) Ricci, J. S.; Koetzle, T. F.; Goodfellow, R. J.; Espinet, P.; Maitlis, P. M. *Inorg. Chem.* **1984**, 23, 1828.

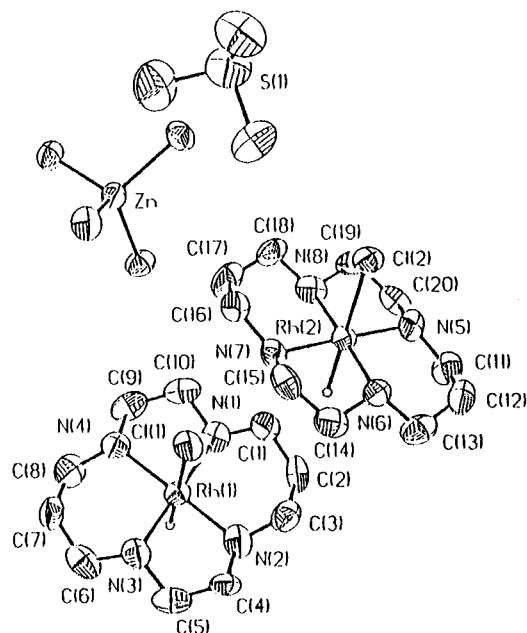
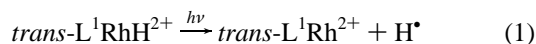


Figure 3. ORTEP drawing of the molecular structure of $\{trans\text{-}(\text{Cl})\text{-}([14]\text{aneN}_4)\text{RhH}\}_2(\text{ZnCl}_4)\cdot\text{dmsO}$. Thermal ellipsoids are drawn at 50% probability.

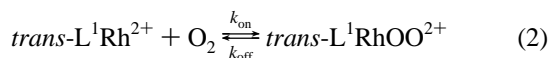
most likely occupies the axial position trans to the chloride, resulting in a pseudooctahedral geometry around the rhodium.

The macrocycle adopts the R,R,S,S configuration, in which two N–H bonds point above and two below the plane of the four nitrogen atoms. The bond lengths and angles within the macrocycle, given in Supporting Information, are close to those found in other metal complexes of L^1 .^{28,29} The rhodium atom is displaced slightly (0.017 Å) toward the coordinated chloride ion.

Generation of $trans\text{-}L^1\text{Rh}(\text{H}_2\text{O})^{2+}$. UV–visible spectra of acidic aqueous solutions of $L^1\text{RhH}^{2+}$ do not change over a period of 24 h at room temperature irrespective of whether O_2 is excluded or not. In contrast to this thermal stability, the photolysis (λ_{irr} 254 nm) of solutions containing submillimolar concentrations of $trans\text{-}L^1\text{RhH}^{2+}$ leads to quantitative homolytic cleavage of the Rh–H bond, eq 1. Gas bubbles, assumed to be molecular hydrogen, were clearly present on the cell walls after photolysis.



The formation of $trans\text{-}L^1\text{Rh}^{2+}$ was confirmed by ESR spectroscopy. Figure 4 shows the spectra obtained after photolysis under Ar and O_2 . The appearance of the spectra and the g and A values identify these two species as the axially symmetric¹⁵ (presumably square pyramidal) $trans\text{-}L^1\text{Rh}(\text{H}_2\text{O})^{2+}$ and axially nonsymmetric^{30,31} $trans\text{-}(\text{H}_2\text{O})L^1\text{RhOO}^{2+}$, the latter undoubtedly produced in the reaction of eq 2. The ESR



parameters are similar to those for the known, related rhodium complexes,^{15,30,31} and have the following values: $trans\text{-}L^1\text{Rh}^{2+}$,

(28) Endicott, J. F.; Lilie, J.; Kuszaj, J. M.; Ramaswamy, B. S.; Schmonsees, W. G.; Sivic, M. G.; Glick, M. D.; Rillema, D. P. *J. Am. Chem. Soc.* **1977**, *99*, 429.

(29) Bakac, A.; Espenson, J. H. *Inorg. Chem.* **1987**, *26*, 4353.

(30) Raynor, J. B.; Gillard, R. D.; Pedrosa de Jesus, J. D. *J. Chem. Soc., Dalton Trans.* **1982**, 1165.

(31) Wayland, B. B.; Newman, A. R. *J. Am. Chem. Soc.* **1979**, *101*, 6472.

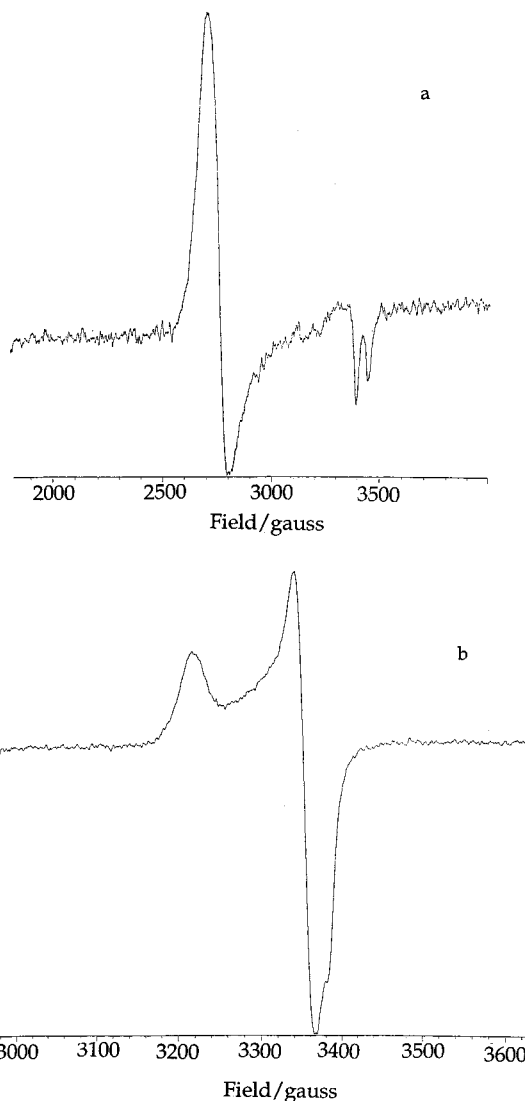


Figure 4. ESR spectra at 120 K of (a) $trans\text{-}(\text{H}_2\text{O})L^1\text{Rh}^{2+}$ and (b) $trans\text{-}(\text{H}_2\text{O})L^1\text{RhOO}^{2+}$ ($L^1 = [14]\text{aneN}_4$) in 0.01 M HClO_4 , $T = 120$ K. $trans\text{-}L^1\text{Rh}^{2+}$, $g_{\parallel} = 1.980$, $A_{\text{Rh}} = 139$ MHz, $g_{\perp} = 2.455$; $trans\text{-}L^1\text{RhOO}^{2+}$, $g_1 = 2.099$, $g_2 = 2.014$, $g_3 = 1.998$.

$g_{\parallel} = 1.980$, $A_{\text{Rh}} = 139$ MHz, $g_{\perp} = 2.455$; $trans\text{-}L^1\text{RhOO}^{2+}$, $g_1 = 2.099$, $g_2 = 2.014$, $g_3 = 1.998$.

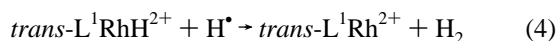
Single-shot laser-flash photolysis of $trans\text{-}L^1\text{RhH}^{2+}$ under Ar did not result in measurable absorbance changes in the UV. This is as expected for reaction 1, because the molar absorptivities of both the reactant and the products are small (Table 3 and Figure 2), and such experiments generate only micromolar levels of products. Attempts were made to demonstrate the formation of hydrogen atoms by their known³² reaction with methyl viologen (MV^{2+}) to produce the strongly colored $\text{MV}^{\bullet+}$ (λ_{max} 600 nm),^{32,33} eq 3.



However, when a solution containing 0.3 mM $trans\text{-}L^1\text{RhH}^{2+}$ was flashed in the presence of 35 μM MV^{2+} , no $\text{MV}^{\bullet+}$ was produced, indicating that another reaction had rapidly consumed H^{\bullet} . We postulate that the reaction of $trans\text{-}L^1\text{RhH}^{2+}$ with H^{\bullet} is responsible, eq 4. This reaction does not introduce any new products, but increases the quantum yields of $trans\text{-}L^1\text{Rh}^{2+}$ and H_2 .

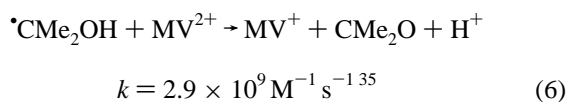
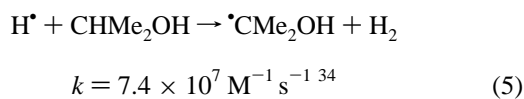
(32) Solar, S.; Solar, W.; Getoff, N.; Holcman, J.; Sehested, K. *J. Chem. Soc., Faraday Trans. 1* **1982**, *78*, 2467.

(33) Watanabe, T.; Honda, K. *J. Phys. Chem.* **1982**, *86*, 2617.

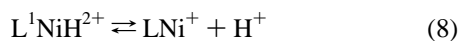


MV²⁺ absorbs strongly at the excitation wavelength (266 nm), which prevented us from increasing the concentration of MV²⁺ to the point where it could compete with *trans*-L¹RhH²⁺ for H[•]. If reaction 4 is indeed the reason for the failure to produce MV⁺, then the rate constant $k_4 > 3 \times 10^8 \text{ M}^{-1} \text{ s}^{-1}$.

The formation of H[•] by the photolysis of *trans*-L¹RhH²⁺ was demonstrated by adding another component, 1.5 M 2-PrOH, to a solution of *trans*-L¹RhH²⁺ and MV²⁺. The large concentration of optically transparent 2-PrOH makes it possible to scavenge hydrogen atoms, produced in reaction 1, and convert them into [•]CMe₂OH radicals,³⁴ which then reduce MV²⁺,³⁵ eqs 5 and 6. At 35 μM MV²⁺, the formation of MV⁺ took place with $k = 1.6 \times 10^5 \text{ s}^{-1}$, in acceptable agreement with the expected³⁵ $1.0 \times 10^5 \text{ s}^{-1}$.



Another test for hydrogen atoms was based on the known reaction between L¹Ni²⁺ and H[•],³⁶ eqs 7 and 8. Under the reaction conditions (0.6 mM L¹Ni⁺, 0.01 M HClO₄), the formation of L¹NiH⁺ in reaction 7 was rapid, and the acid–



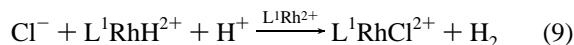
base equilibrium of eq 8 dominated the observed chemistry. Following the laser pulse, a kinetic trace at 380 nm matched closely that reported,³⁶ and the observed rate constant for the absorbance increase, $(1.2 \pm 0.2) \times 10^6 \text{ s}^{-1}$, was acceptably close to that calculated,³⁶ $k_{8,\text{calc}} = (8.3 \pm 1.7) \times 10^5 \text{ s}^{-1}$. The photochemistry of eq 1 has thus been established by observing the chemistry of hydrogen atoms and by the direct observation of the rhodium(II) product. The photolysis of the Rh–H

bond in the related *trans*-(NH₃)₄(H₂O)RhH²⁺ has been invoked earlier,³⁷ although the products have not been observed.

The Lifetime of *trans*-L¹Rh²⁺. A solution of *trans*-L¹RhH²⁺ (0.2 mM) in 0.05 M HClO₄ was photolyzed for 90 s in a Rayonet reactor. After the desired period of time, an aliquot was injected into O₂-saturated 5 mM HClO₄ (final [H⁺] = 0.02 M), and the UV spectrum recorded. The intensity of the maximum at 270 nm, corresponding to L¹RhOO²⁺, was taken as a measure of the concentration of L¹Rh²⁺ in the photolyzed solution. Even after the solution had been aged for half an hour, there was still ~50% *trans*-L¹Rh²⁺ present in solution. Thus the nonplanarity of the macrocycle causes sufficient crowding around the rhodium to prevent metal–metal bond formation. We are not certain whether the eventual loss of *trans*-L¹Rh²⁺ is caused by demetalation or by a slow air leak. In either event, it is clear that Rh(II) is sufficiently long-lived to be used for kinetic and mechanistic studies, some of which are already under way in our laboratory.

From our present estimate for the molar absorptivity of L¹-RhOO²⁺, $\epsilon_{270} = (5.5 \pm 1.5) \times 10^3 \text{ M}^{-1} \text{ cm}^{-1}$, we calculate that ≥60% of the initially present *trans*-L¹RhH²⁺ was converted to *trans*-L¹Rh²⁺ during the 90-s irradiation.

When chloride ions were present during the photolysis, Rh(II) was not observed. Instead, the mono- and dichlororhodium(III) complexes were produced, along with hydrogen gas. Apparently, the Rh(II)-catalyzed aqutation of the hydride takes place, and chloride ions facilitate the reaction, eq 9. Halide ions are



efficient bridging ligands in many aquations induced by reduced metals. A similar reaction has been observed earlier¹⁶ in the related Rh(NH₃)₄²⁺/*trans*-(Br)₂Rh(NH₃)₄⁺ system.

Acknowledgment. We thank Drs. R. Jacobson and J. H. Espenson for helpful comments, Dr. Stan Bajic for help in obtaining the infrared spectra, Dr. W.-D. Wang for help with NMR spectroscopy, and Dr. R. Kniseley for running the ICP analyses of rhodium. This work was supported by the U.S. Department of Energy, Office of Basic Energy Sciences, Division of Chemical Sciences under Contract W-7405-Eng-82.

Supporting Information Available: Complete tabular information on collection of data and refinement of structure, listings of all angles and distances, anisotropic thermal parameters, and the derived hydrogen positions, and a table of least squares planes and deviations therefrom (16 pages). Ordering information is given on any current masthead page.

IC960300A

(34) Buxton, G. V.; Greenstock, C. L.; Helman, W. P.; Ross, A. B. *J. Phys. Chem. Ref. Data* **1988**, *17*, 513.

(35) Venturi, M.; Mulazzani, Q. G.; Ciano, M.; Hoffman, M. Z. *Inorg. Chem.* **1986**, *25*, 4493.

(36) Kelly, C. A.; Mulazzani, Q. G.; Venturi, M.; Blinn, E. L.; Rodgers, M. A. *J. Am. Chem. Soc.* **1995**, *117*, 4911.

(37) Endicott, J. F.; Wong, C.-L.; Inoue, T.; Natarajan, P. *Inorg. Chem.* **1979**, *18*, 450.